Available online at www.sciencedirect.com
ScienceDirect
Journal of Power Sources 173 (2007) 972–978
JOURNAL OF POWER SOURCES
www.elsevier.com/locate/jpowsour

Short communication

Proton and hydrogen formation by cyclohexyl benzene during overcharge of Li-ion batteries

Hochun Lee, Soojin Kim, Jongho Jeon, Jeong-Ju Cho *

Batteries R&D, LG Chem Ltd., 104-1 Moonji-dong, Yuseong-gu, Daejeon 305-380, South Korea

Received 7 May 2007; received in revised form 14 August 2007; accepted 21 August 2007
Available online 1 September 2007

Abstract

This study provides experimental evidence for proton and hydrogen formation caused by the anodic electropolymerization of cyclohexyl benzene (CHB), which is a popular electrolyte additive for overcharge protection of lithium-ion batteries (LIBs). It is found that considerable H_2 evolution is observed in overcharged $LiCoO_2$/graphite cells, especially when CHB is included as an electrolyte additive. In order to confirm the proton generation during the CHB oxidation, Pt/Pt-rotating ring disc electrode (RRDE) measurements are performed in 1 M $Li(C_2F_5SO_2)_2N$ ethylene carbonate/ethyl methyl carbonate (1/2, v/v) solutions with and without CHB. The cathodic ring current is intimately correlated to the anodic disc current, and the cathodic reaction at the ring is determined to be the reduction of the proton. The proton generation efficiency during the CHB oxidation is as high as 90%. Proton liberation is also observed during the anodic decomposition of the electrolyte solvents, although it occurs in a much less stoichiometric way compared with that during the CHB oxidation.

Keywords: Cyclohexyl benzene; Proton; Hydrogen; Lithium-ion battery; Overcharge; Rotating ring disc electrode

1. Introduction

Overcharging has long been the safety problem of most concern for lithium-ion batteries (LIBs). Aromatic compounds such as cyclohexyl benzene (CHB) and biphenyl (BP) are being widely employed as electrolyte additives for overcharge protection of LIBs [1–6]. However, there still remains some ambiguity on their operating mechanism. It has been claimed that they are oxidized to form a passive polymeric film at the cathode|electrolyte interface, which hinders Li ion transport and eventually prevents additional charging of LIBs [5,6]. The additives have also been suggested to generate H_2 gas during the process of the anodic polymerization, which increases the internal pressure to activate the current interrupt device (CID) of cylindrical LIBs [1–4].

Scheme 1 depicts the detailed mechanism of the anodic electropolymerization of CHB based on the radical coupling mechanism [7–9]. Shima et al. [1] have recently reported that bond formation between aromatic monomers such as BP and CHB is preferred at *ortho*-positions of the phenyl groups. The scheme predicts that two H^+ ions are generated for every bond formation between phenyl groups. Regarding H_2 evolution resulting from the aromatic additives during the overcharge, it has been suggested that H^+ is liberated from the oxidized species, moves to the anode side, and is then reduced to H_2 gas [1,5,6]. To date, however, there has been no solid experimental support for the interplay between the cathode and the anode. This appears to be due mainly to the difficulty in detecting protons in non-aqueous LIB electrolytes.

Determination of the H^+ concentration in LIB electrolytes is not as straightforward as in aqueous solutions. Acid–base titration with a strong base, e.g., concentrated NaOH solution, is usually conducted for water-diluted LIB electrolytes, which is indirect and defective in nature. Recently, Beck and co-workers [10,11] have employed the rotating ring disc electrode (RRDE) technique to monitor H^+ generation during the oxidation of aprotic non-aqueous electrolytes. Using the RRDE technique, the reaction product at the disc electrode can be electrochemically determined at the ring electrode by adjusting each electrode potential [12]. The RRDE technique has also been found to be a very versatile tool for the study of

* Corresponding author. Tel.: +82 42 866 2512; fax: +82 42 866 2934.
E-mail address: chojj@lgchem.com (J.-J. Cho).

0378-7753/$ – see front matter © 2007 Elsevier B.V. All rights reserved.
doi:10.1016/j.jpowsour.2007.08.061

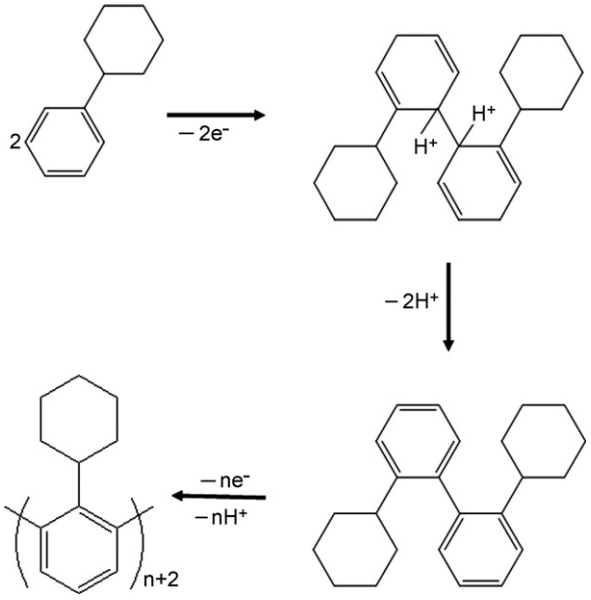

Scheme 1. Proposed mechanism of anodic electropolymerization of CHB.

the reductive decomposition of LIB electrolytes [13] and Mn dissolution from Mn-based cathodes [14].

This study aims to investigate H^+ liberation during the oxidation of LIB electrolytes by means of gas analysis and the RRDE technique. First, the H_2 evolution in overcharged $LiCoO_2$/graphite cells with and without CHB is investigated by means of gas chromatography with a mass selective detector (GC–MS). Then, the RRDE measurements are performed to monitor the H^+ generation during the oxidation of 1 M $Li(C_2F_5SO_2)_2N$ (LiBETI) in ethylene carbonate (EC)/ethyl methyl carbonate (EMC) (1/2, v/v) solution with and without CHB. For this purpose, the redox potential of the H_2/H^+ couple on a Pt electrode in the electrolytes containing various acids are determined for comparison.

2. Experimental

2.1. Chemicals and cell preparation

Battery grade 1 M $LiPF_6$ and 1 M $Li(C_2F_5SO_2)_2N$ (LiBETI) in ethylene carbonate (EC)/ethyl methyl carbonate (EMC) (1/2, v/v) were used as the base electrolyte solutions for cell manufacture and electrochemical experiments, respectively. The water content in each of the electrolytes was determined using the Karl–Fisher titration method at less than 20 ppm. The free acid contents in the electrolytes were 50 and less than 2 ppm, respectively. Reagent grade HF (48 wt.% in water), HCl (37 wt.% in water), $HClO_4$ (70% ACS specification), and CF_3SO_3H (99%) were used. Cyclohexyl benzene (98%, Acros) was purified to more than 99.9% by vacuum distillation prior use. $LiCoO_2$/graphite Al-laminated pouch cells (383562-size, 700 mAh) were employed for the gas analysis. Mesocarbon microbeads graphite (Osaka gas, Japan) was used as an anode material and $LiCoO_2$ (NCI, Japan) as a cathode material, with polyethylene as the separator (Tonen, Japan). The electrolyte was 1 M $LiPF_6$ in a mixture of EC/EMC (1/2, v/v). Three types of $LiCoO_2$/graphite cells were charged at a 0.1 C constant current to 4.2 V. One of them was analyzed as-prepared. The other two types were opened and degassed inside the vacuum chamber in order to eliminate the gases evolved on the first charge (formation gases). They were then cycled several times over 3–4.2 V and overcharged for 90 min with a 1 C current before gas analysis. One of the overcharged cells contained 5 wt.% CHB in the electrolyte.

2.2. Instrumentation

Gas chromatography (HP 6890A) was coupled to a mass selective detector (HP 5973) for examining gas composition, and to a thermal conductive detector for measuring the amounts of individual components.

A three-electrode configuration was employed for all electrochemical experiments. The reference electrode was Li foil and the counter electrode was Pt wire. A Pt disc (area = 0.02 cm^2) served as the working electrode for the determination of H_2/H^+ potential and the cyclic voltammetry of CHB. The working electrode for the rotating ring disc electrode (RRDE) experiments was a Radiometer model EAD10000 in which the Pt disc has a radius of 2.0 mm (area = 0.13 cm^2) and Pt ring radii of 2.2 and 2.4 mm (area = 0.03 cm^2). Electrochemical experiments were carried out with a VoltaLab 40 (Radiometer). For RRDE experiments, two potentiostats (Radiometer, VoltaLab 10 and VoltaLab 40) were combined to serve as a bipotentiostat and rotation was performed with a rotor (Radiometer, Tachyprocesseur). In RRDE experiments, the collection efficiency (N) is defined as [11]:

$$N = \left(\frac{r_3^3}{r_1^3} - \frac{r_2^3}{r_1^3}\right)^{2/3} = -\left(\frac{i_R}{i_D}\right) \quad (1)$$

where i_R is the ring current, i_D the disc current, r_3 the outer ring radius, r_2 the inner ring radius, and r_1 is the disc radius. The geometry of the RRDE used in this study predicts the theoretical N value to be 0.54. In order to determine the N value experimentally, the ratio of i_R to i_D was obtained for a ferrocene ($Fc^{0/+}$) couple. Ferrocene is well known as a standard material with an invariant redox potential and ideal chemical reversibility [15]. The ring electrode was held at 3.1 V, while the disc electrode was swept from 3.1 to 3.6 V in 5 mM ferrocene in the LiBETI solution. The ratio of i_R to i_D was about 0.15 over a rotation speed from 100 to 1600 rpm, which is much smaller than the theoretical one. This difference appears to be mainly due to imperfect flatness between the disc and the ring, which hinders lamina flow from the disc to the ring. It is believed that the experimental N value can be considered as a practical one.

Preparation of electrolytes and all the electrochemical experiments were performed in an argon-atmosphere glove box in which H_2O and O_2 concentrations were kept below 5 ppm and the temperature was held at 25 ± 2 °C.

Table 1
Gas amounts (arbitrary units) in $LiCoO_2$/graphite cells

Cells	H_2	C_2H_4	CO	CO_2	CH_4	C_2H_6	Others
Initial charged cell	0.25	1.85	0.37	0.05	0.05	0.03	0.02
Overcharged cell	2.19	0.06	0.02	0.23	1.40	2.42	0.19
Overcharged cell with CHB	3.75	0.46	0.02	0.79	0.14	1.05	1.03

3. Results and discussion

3.1. Hydrogen evolution in overcharged $LiCoO_2$/graphite cells

The gas composition of three $LiCoO_2$/graphite cells treated in different ways is shown in Table 1. The listed numbers are the values in arbitrary units derived from the detector signals, which are proportional to the amounts of gas species. The gas amounts in the initial charged cell are in the following order: $C_2H_4 > CO > H_2 > CO_2 = CH_4 > C_2H_6$. It is generally accepted that SEI formation at the graphite anode is mainly responsible for gas evolution during the first charging process [16,17]. C_2H_4 is known to result from EC reduction, whereas CH_4 and C_2H_6 arise from EMC reduction. CO_2 and CO can be traced to either EC or EMC [16–19]. H_2 gas evolved in the first charge is usually assigned to the reduction of trace water present in the electrolytes [18–20].

Not only are the overall amounts of the evolved gases greatly increased in the overcharged cells, but the composition of the gas species is also very different when compared with that in a normally charged cell. The order of gas amounts in the overcharged cell without CHB is $C_2H_6 > H_2 > CH_4 > CO_2 > C_2H_4$. Note the large quantity of H_2 gas in the overcharged cells. Intensive H_2 evolution during overcharge has also been observed in other reports, but no explanation has been given [2,21]. Obviously, the large amount of H_2 can hardly be attributed to the trace water present as an impurity in the cell. H_2 content is greater when CHB is included as an electrolyte additive. There has also been a previous observation of large amounts of H_2 in an overcharged cell containing CHB [2]. It is frequently reported that CO_2 is a major gas component in overcharged LIBs [22,23], which is not the case in this study. It is considered that several factors such as cell design, overcharge conditions, and analysis method may affect the gas composition in overcharged LIBs [20].

When '4-V class' LIBs are overcharged, the cathode voltage is increased to be sufficiently high to cause electrolyte oxidation (>4.5 V versus Li/Li^+). Beck and his co-workers [10,11] have suggested the possibility of H^+ generation during the oxidation of organic solvents. They performed RRDE experiments with propylene carbonate and acetonitrile solutions with 0.2 M $LiClO_4$. However, the water concentration in their electrolytes was rather high (about 300 ppm) so that H^+ may be generated from the water rather than the organic solvents. In addition, the high water content may facilitate the decomposition of organic solvents and affect the reaction pathways [24–27]. Meanwhile, it is also possible that the active Li metal deposited on the overcharged anode may enhance the reductive decomposition of the electrolyte and result in the evolution of H_2 gas. Indeed, it has been reported that H_2 was the one of the major gas components present in coin-type half-cells employing Li metal [16]. All the above ambiguities provide a motive to seek direct evidence for H^+ formation during the oxidation of LIB electrolytes under conditions where the water content is strictly controlled.

3.2. Determination of redox potential of H_2/H^+ in 1 M LiBETI EC/EMC

To our best knowledge, there has been no systematic study of the redox reaction of the H_2/H^+ couple in a non-aqueous LIB electrolyte. Fig. 1 compares the cyclic voltammograms (CVs) of 1 M LiBETI EC/EMC (1/2, v/v) solutions containing various acids such as CF_3SO_3H (1.0 mM), $HClO_4$ (4.2 mM), HCl (3.0 mM), and HF (13.5 mM). The water content of the acid solutions was determined as 1.4, 11.3, 11.8, and 19.7 mM, respectively. The potentials of the redox couples in Fig. 1 are in the range of 2.8–3.2 V, depending on the kind of acid used. The redox potential of the standard hydrogen electrode (SHE) is 3.05 V on the Li/Li^+ scale [12], while the reduction potential of water in non-aqueous solutions has been reported to be as low as 1.8 V [28,29]. Thus, the redox reactions shown in Fig. 1 can be reasonably assigned to the H_2/H^+ couples. It can be anticipated that the water content in non-aqueous media may affect H_2/H^+ potential. Higher amounts of water are expected to enhance the dissociation of the acid so that it shifts the H_2/H^+ potential in a positive direction. However, as shown in Fig. 1, the order of the H_2/H^+ potentials is reverse to that of the water content in the acid

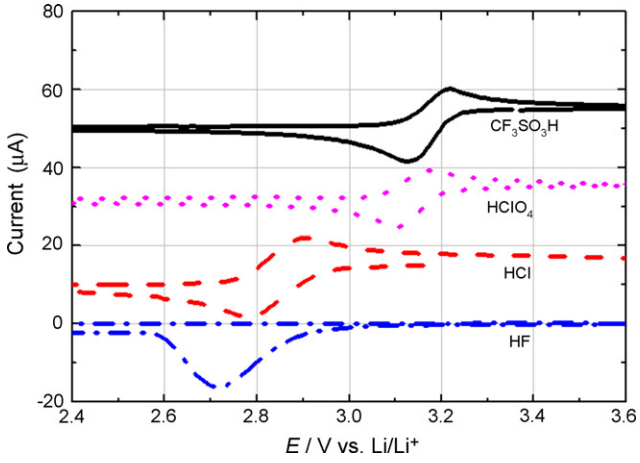

Fig. 1. First CVs in 1 M LiBETI EC/EMC (1/2, v/v) containing CF_3SO_3H (1 mM, solid), $HClO_4$ (4.2 mM, dot), HCl (3 mM, dash), and HF (13.5 mM, dash dot). Pt (area = 0.02 cm^2) as a working electrode. Scan rate = 20 mV s^{-1}.

solutions, and the correlation between them seems rather weak. Therefore, the variation in H_2/H^+ potentials observed in Fig. 1 appear to be more related to the nature of the acids. Due to the soft characteristic of the conjugate anion, CF_3SO_3H is supposed to release H^+ ions easily compared with other acids, which would lead to a most positive H_2/H^+ potential. By contrast, HF exhibits the most negative reduction potential and the corresponding re-oxidation peak is absent. In our previous study [30], the notable behaviour of HF has been ascribed to the formation of a LiF precipitate that acts as a passive layer towards the cathodic reactions below 3 V versus Li/Li^+. This implies that electrolyte solutions with $LiPF_6$ salt, which is inevitably contaminated with a trace of HF, are not a suitable medium for determining the redox reaction of the H_2/H^+ couple. This is the reason why LiBETI has been chosen as the electrolyte salt, instead of $LiPF_6$, in this study.

3.3. Voltammetric behaviour of CHB

Fig. 2 shows two consecutive voltammograms for a Pt disc electrode in 1 M LiBETI EC/EMC (1/2, v/v) solution with 3 wt.% CHB. On the first cycle, the oxidation current starts to increase above 4.8 V and displays a couple of peaks between 5.1 and 5.3 V. The oxidation current for the base electrolyte (without CHB) is negligible up to 5.5 V (not shown here). The current on the second anodic scan in the CHB solution starts to increase as early as 4.2 V and attains a much higher value than that during the first scan. A dark brown film is observed on the surface of the Pt electrode after the CV scans. The enhanced anodic reactivity during the subsequent scans has been attributed to the oxidation products that are more easily oxidizable than the original monomer [1,2]. It has also been suggested that a poly-CHB film formed on the first cycle accelerates further electropolymerization [6]. Note that there is a relatively small redox couple at 3.0–3.4 V around the end of the first cycle and the beginning of the second cycle (Fig. 2b). It appears that the redox reaction is related to the oxidation products of CHB since it is absent before the first anodic scan and its current is increased on the second cycle. It can be concluded that oligo-CHB or some radical cations residing near the electrode surface may be responsible for the new peak. However, it has been shown from both experiments and quantum chemical calculations that possible oxidation products such as alkyl benzene, terphenyl, and their derivatives exhibit oxidation potentials higher than 3.5 V [1,2,31–37]. Thus, it is expected that the new redox couple is due to H^+ ions liberated during the CHB oxidation. This is confirmed in following section.

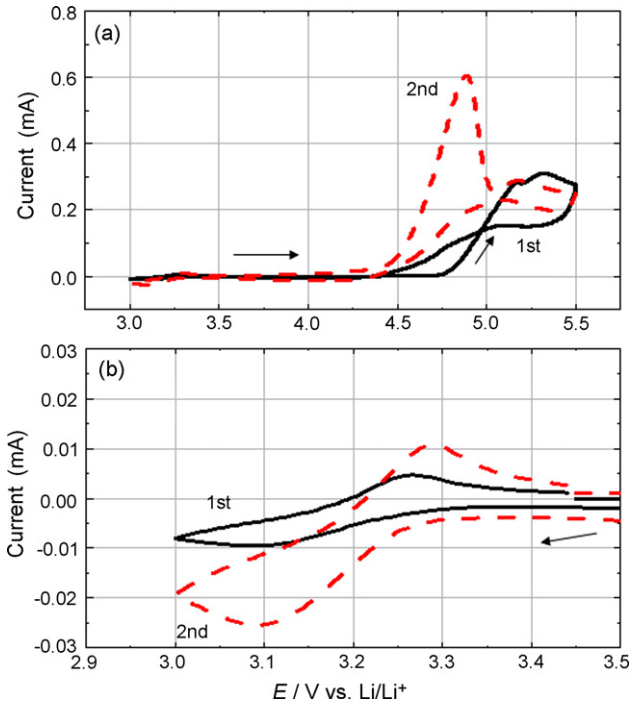

Fig. 2. Two consecutive CVs in 1 M LiBETI EC/EMC (1/2, v/v) containing 3 wt.% CHB. First cycle (solid) and second cycle (dash). (a) Overall and (b) enlarged views. Pt (area = 0.02 cm^2) as a working electrode. Scan rate = 20 mV s^{-1}.

3.4. Proton generation during CHB oxidation

In order to investigate H^+ liberation during CHB oxidation, rotating disc electrode (RDE) and the rotating ring disc electrode (RRDE) experiments were performed. Fig. 3 presents a linear sweep voltammogram (LSV) of a Pt disc rotating at a speed of 400 rpm in a 1 M LiBETI EC/EMC (1/2, v/v) solution with and without CHB. As the disc potential is linearly swept from 3.5 to 6 V, the oxidation current in the CHB solution (thick line) begins to flow at around 4.8 V as in the stationary case (Fig. 2a). This indicates that the onset potential for CHB oxidation is not affected by the forced convection. However, the current steadily rises up to 6 V unlike that in Fig. 2a. This implies that the CHB oxidation is a diffusion-limited reaction in a stationary condition, while it is kinetic-controlled under a hydrodynamic condition. When CHB is not present in the electrolyte, the anodic current remains negligible up to 5.8 V (thin line in Fig. 3).

The RRDE experiments were performed with a CHB solution (Fig. 4). A constant current was applied to the disc and the ring potential was linearly scanned in the cathodic direction from 3.5 to 2.0 V. As shown in Fig. 4a, the ring current (i_R) dis-

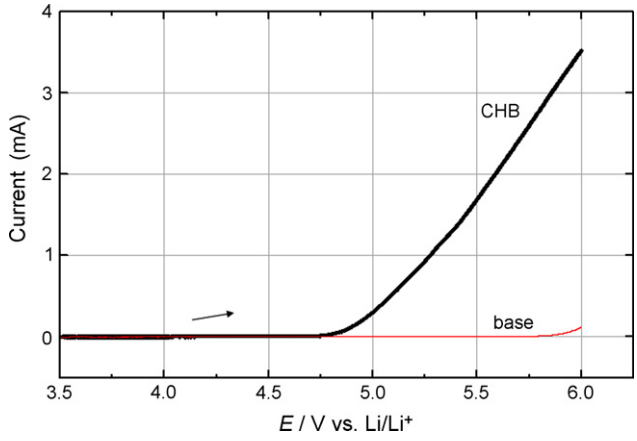

Fig. 3. LSVs of 1 M LiBETI EC/EMC (1/2, v/v) containing 2 wt.% CHB (thick line) and without CHB (thin line). Rotating speed = 400 rpm. Pt (area = 0.13 cm^2) as a working electrode. Scan rate = 20 mV s^{-1}.

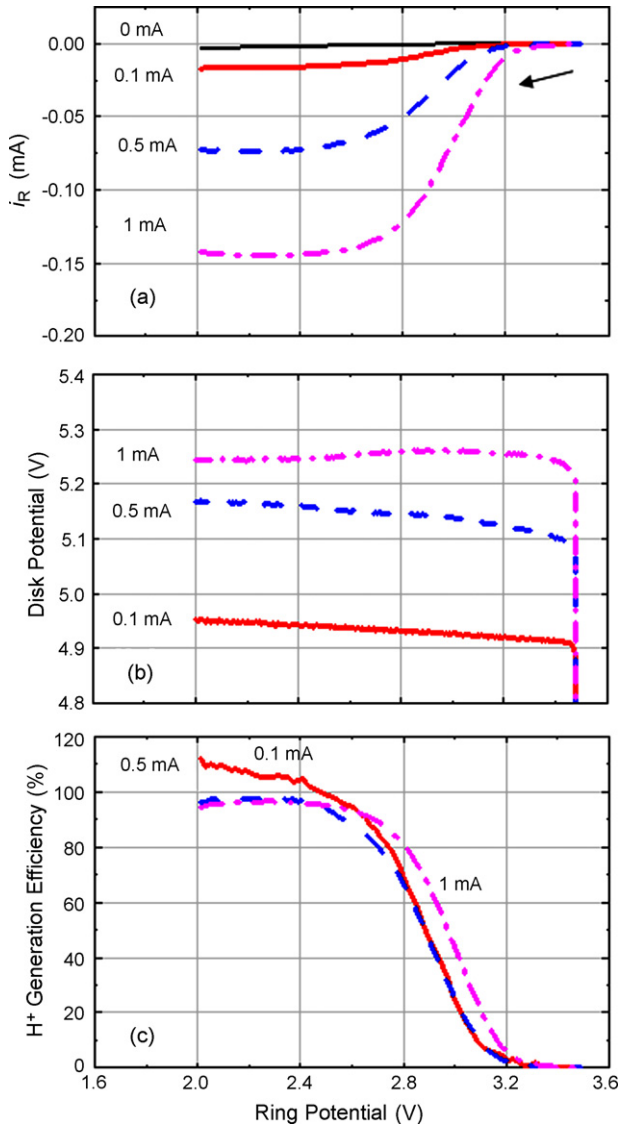

Fig. 4. RRDE results with a constant disc current of 0 mA (thin solid), 0.1 mA (solid), 0.5 mA (dash), and 1 mA (dash dot) in 1 M LiBETI EC/EMC (1/2, v/v) containing 2 wt.% CHB. Rotating speed = 400 rpm. (a) Currents at the ring that is linearly swept at 10 mV s^{-1}, (b) disc potentials, and (c) concurrent plots of the H^+ generation efficiency defined in Eq. (2).

plays sigmoidal behaviour, and the limiting i_R increases with the disc current (i_D). The disc potential also increases with i_D over 4.9–5.3 V, which is above the onset potential for CHB oxidation observed in Fig. 3. Note that the half-wave potential for the i_R in Fig. 4a is around 2.9–3.0 V, which is within the range of the H_2/H^+ potential observed in Fig. 2. These results clearly indicate that the cathodic reaction at the ring is due to the reduction of H^+ ions generated from CHB oxidation at the disc. The efficiency of proton generation (α) can be defined as:

$$\alpha = -\frac{i_R - i_{Ro}}{N\, i_D} \times \varepsilon_Q \times 100 \qquad (2)$$

where i_{Ro} is the background ring current as the i_D is zero, N the collection efficiency of the RRDE electrode as explained above, and ε_Q the current efficiency defined as the ratio of the charge consumed to oxidize CHB to the total charge delivered. Plots of α value versus ring potential are given in Fig. 4c. The plots for different i_D values are similar, which implies that the nature of the reduction occurring at the ring, and thus the oxidation at the disc, is hardly altered within the tested i_D values. Note that the α value is more than 90% over the limiting i_R region (<2.4 V). An α value of 100% means that every bond formation between phenyl groups liberates two H^+ ions. In our previous study [6], the coulombic efficiency of CHB polymerization was determined as 85% over 5–5.5 V, as proven by measurements with an electrochemical quartz crystal microbalance (EQCM). Accordingly, the α value higher than 90% in this study appears to be reasonable. In case of i_D = 0.1 mA, the α value goes beyond 100% as the ring potential is less than 2.5 V. It is concluded that this is probably due to the experimental error in measuring the background current (i_{Ro}), the effect of which becomes rather adverse when the i_R is relatively low.

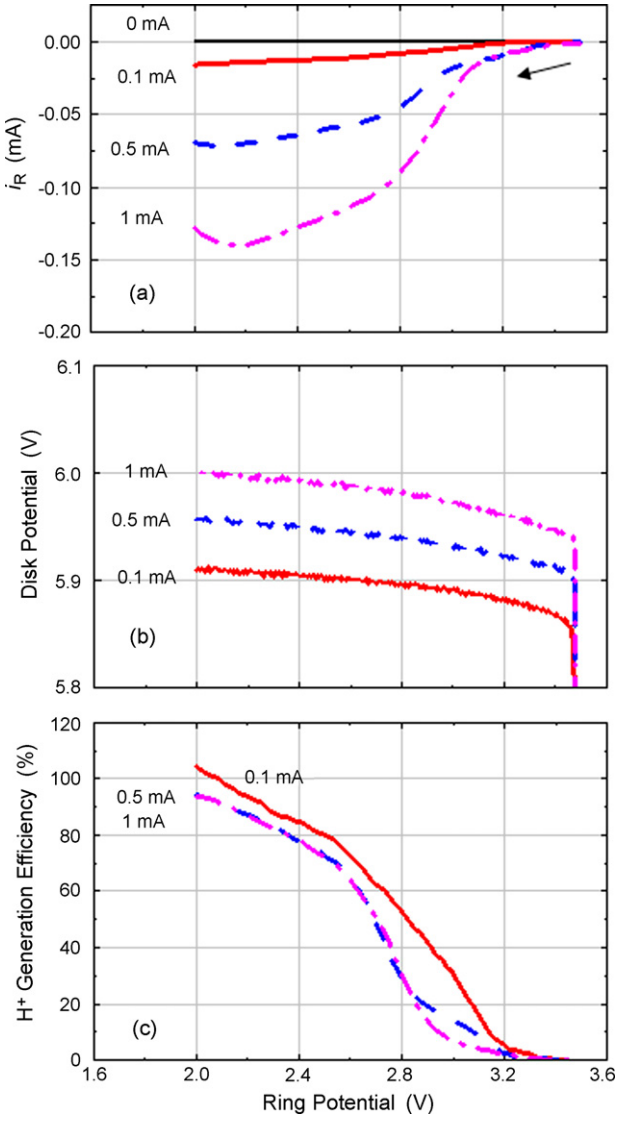

Fig. 5. RRDE results with constant disc current of 0 mA (thin solid), 0.1 mA (solid), 0.5 mA (dash), and 1 mA (dash dot) in 1 M LiBETI EC/EMC (1/2, v/v). Rotating speed = 400 rpm. (a) Currents at the ring that is linearly swept at 10 mV s^{-1}, (b) disc potentials, and (c) concurrent plots of the H^+ generation efficiency defined in Eq. (2).

3.5. Proton generation during oxidation of 1 M LiBETI EC/EMC

The same RRDE experiment as that in Fig. 4 was repeated for a solution without CHB (Fig. 5). The i_R curves in Fig. 5a have slanted sigmoidal shapes. Although not so clear as in the CHB case, the rapid increase in i_R over 3.2–2.8 V can be reasonably assigned to the H^+ reduction based on its potential range. Thus, besides H^+ reduction, there appears to exist additional cathodic reactions that cause the sloped sigmoid behaviour of the i_R. The disc potential is in the range of 5.8–6.0 V (Fig. 5b), which is consistent with the LSV result shown in Fig. 3. Various authors have reported the presence of CO_2 evolution during the oxidation of LIB electrolytes [20,24,26,38,39], but the electrochemical reduction of CO_2 in aprotic media is well known to be negligible above 2 V (vs. Li/Li^+) [40–42]. Aurbach and his co-workers [43] have recently reported that the anodic decomposition of carbonate solvents may yield various carbonyl compounds such as aldehydes, esters, and CO. It has also been claimed [44] that some organic radicals can be formed as a result of the anodic reactions of linear and cyclic carbonates. Therefore, it is assumed that some of the chemical species mentioned above are responsible for the additional cathodic reaction at the ring. The α value in Fig. 5c is much less than that in the CHB, which should be due to oxidation reactions that do not liberate H^+ ions. Obviously, H^+ liberation should result from the anodic decomposition of EC and EMC rather than from the salt (LiBETI). At present, however, it is difficult to determine the relative contributions of EC and EMC to the overall anodic current and H^+ generation. Experiments with solutions employing a single solvent or deuterium-substituted solvents may be able to reveal the respective contributions. Some of these studies are in progress in our group. In summary, it is quite probable that the anodic decomposition of the electrolyte solvents is accompanied by H^+ generation, although in a much less stoichiometric manner than with CHB oxidation.

4. Conclusions

It has been demonstrated that a proton is generated during the electropolymerization of CHB, a popular electrolyte additive for overcharge protection of LIBs. It is also suggested that the anodic decomposition of the electrolyte solvents is accompanied by some proton generation. These results shed some light on the following two issues: (i) the working mechanism of CHB as an overcharge protector involves CHB oxidation at the cathode that generates a proton, which is reduced to hydrogen gas at the anode, and finally turns on the current interrupting device of cylindrical LIBs; (ii) rigorous build-up of hydrogen gas within LIBs subject to overcharge abuse is at least partly ascribed to the anodic decomposition of electrolyte solvents.

References

[1] K. Shima, K. Shizuka, M. Ue, H. Ota, T. Hatozaki, J.-I. Yamaki, J. Power Sources 161 (2006) 1264–1274.
[2] K. Shima, M. Ue, J. Yamaki, Electrochemistry 71 (2003) 1231–1235.
[3] S. Tobishima, Y. Ogino, Y. Watanabe, J. Appl. Electrochem. 33 (2003) 143–150.
[4] L. Xiao, X. Ai, Y. Cao, H. Yang, Electrochim. Acta 49 (2004) 4189–4197.
[5] X. Feng, X. Ai, H. Yang, J. Appl. Electrochem. 34 (2004) 1199–1203.
[6] H. Lee, J. Lee, S. Ahn, H.-J. Kim, J.-J. Cho, Electrochem. Solid State Lett. 9 (2006) A307–A310.
[7] C. Kvarnström, R. Bliger, A. Ivaska, J. Heinze, Electrochim. Acta 43 (1998) 355–366.
[8] L.M. Goldenberg, P.C. Lacaze, Synthetic Met. 58 (1993) 271–293.
[9] M. Satoh, K. Imanishi, K. Yoshino, J. Electroanal. Chem. 317 (1991) 139–151.
[10] R. Chromik, F. Beck, Electrochim. Acta 45 (2000) 2175–2185.
[11] T. Boinowitz, F. Beck, J. Electroanal. Chem. 461 (1999) 167–173.
[12] A.J. Bard, L.R. Faulkner, Electrochemical Methods: Fundamentals and Applications, 2nd ed., John Wiely & Sons, New York, 2001, pp. 331–367.
[13] E. Endo, K. Tanaka, K. Sekai, J. Electrochem. Soc. 147 (2000) 4029–4033.
[14] L.-F. Wang, C.-C. Ou, K.A. Striebel, J.-S. Chen, J. Electrochem. Soc. 150 (2003) A905–A911.
[15] G. Gritner, J. Kuta, Pure Appl. Chem. 56 (1984) 461–466.
[16] H. Ota, T. Akai, M. Kotaro, S. Yamaguchi, Meeting Abstracts 42nd Battery Symposium in Japan, Yokohama, November 21–23, 2001, 3C20.
[17] H. Yoshida, T. Fukunaga, T. Hazama, M. Terasaki, M. Mizutani, M. Yamachi, J. Power Sources 68 (1997) 311–315.
[18] M.R. Wagner, P.R. Raimann, A. Trifonova, K.-C. Moeller, J.O. Besenhard, M. Winter, Electrochem. Solid State Lett. 7 (2004) A201–A205.
[19] R. Imhof, P. Novak, J. Electrochem. Soc. 145 (1998) 1081–1087.
[20] G. Eggert, J. Heitbaum, Electrochim. Acta 31 (1986) 1443–1448.
[21] T. Ohsaki, T. Kishi, T. Kuboki, N. Takami, N. Shimura, Y. Sato, M. Sekino, A. Satoh, J. Power Sources 146 (2005) 97–100.
[22] K. Kumai, H. Miyashiro, Y. Kobayashi, K. Takei, R. Ishikawa, J. Power Sources 81–82 (1999) 715–719.
[23] A. Negishi, Y. Saito, K. Takano, K. Kato, K. Nozaki, Electrochemistry 71 (2003) 1102–1104.
[24] F. Joho, P. Novak, Electrochim. Acta 45 (2000) 3589–3599.
[25] P. Krtil, L. Kavan, P. Novak, J. Electrochem. Soc. 145 (1993) 3390–3395.
[26] B. Rasch, E. Cattaneo, P. Novak, W. Vielstich, Electrochim. Acta 36 (1991) 1397–1402.
[27] D. Aurbach, H. Gottlib, Electrochim. Acta 34 (1989) 141–156.
[28] D. Aurbach, M. Daroux, P. Faguy, E. Yeager, J. Electroanal. Chem. 297 (1991) 225–244.
[29] J.S. Gnanaraj, M.D. Levi, Y. Gofer, D. Aurbach, M. Schmidt, J. Electrochem. Soc. 150 (2003) A445–A454.
[30] H. Lee, J.-J. Cho, J. Kim, H.-J. Kim, J. Electrochem. Soc. 152 (2006) A1193–A1198.
[31] Y. Watanabe, H. Morimoto, S. Tobishima, J. Power Sources 154 (2006) 244–246.
[32] Y.-K. Han, J. Jung, J.-J. Cho, H.-J. Kim, Chem. Phys. Lett. 368 (2003) 601–608.
[33] H. Lee, S.-Y. Cui, S.-M. Park, J. Electrochem. Soc. 148 (2001) D139–D145.
[34] J.K. Feng, X.P. Ai, Y.L. Cao, H.X. Yang, Electrochem. Commun. 9 (2007) 25–30.
[35] Z. Chen, Q. Wang, K. Amine, J. Electrochem. Soc. 153 (2006) A2215–A2219.
[36] C. Buhrmester, J. Chen, L. Moshurchak, J. Jiang, R.L. Wang, J.R. Dahn, J. Electrochem. Soc. 152 (2005) A2390–A2399.
[37] M. Adachi, K. Tanaka, K. Sekai, J. Electrochem. Soc. 146 (1999) 1256–1261.
[38] R. Imhof, P. Novak, J. Electrochem. Soc. 146 (1999) 1702–1706.
[39] J. Vetter, M. Holzapfel, A. Wuersig, W. Scheifele, J. Ufheil, P. Novak, J. Power Sources 159 (2006) 277–281.
[40] S.E. Sloop, J.B. Kerr, K. Kinoshita, J. Power Sources 119–121 (2003) 330–337.

[41] G.A. Dawson, P.C. Hauser, P.A. Kilmartin, G.A. Wright, Electroanalysis 12 (2000) 105–110.
[42] P.J. Welford, B.A. Brookes, J.D. Wadhawan, H.B. McPeak, C.E.W. Hahn, R.G. Compton, J. Phys. Chem. B 105 (2001) 5253–5261.
[43] M. Moshkovich, M. Cojocaru, H.E. Gottlieb, D. Aurbach, J. Electroanal. Chem. 497 (2001) 84–96.
[44] X. Zhang, J.K. Pugh, P.N. Ross, J. Electrochem. Soc. 148 (2001) E183–E188.